Supporting Information

A coumarin coupled tetraphenylethylene based multi targeted AIE-gen for cyanide ion and nitro explosive detection, and cellular imaging

Viraj G. Naik,[a] Sharanabasava D. Hiremath,[a] Ankit Thakuri,[a] Vijay Hemmadi,[b] Malabika Biswas,[b] Mainak Banerjee *[a] and Amrita Chatterjee*[a]

[a]Department of Chemistry and [b]Department of Biological Sciences BITS, Pilani K K Birla Goa Campus, NH 17B Bypass Road, Zuarinagar, Goa 403726, India.

Corresponding authors e-mail: amrita@goa.bits-pilani.ac.in; mainak@goa.bits-pilani.ac.in

Table of contents

1. Solid-state emission images of the probe TPE-Lac

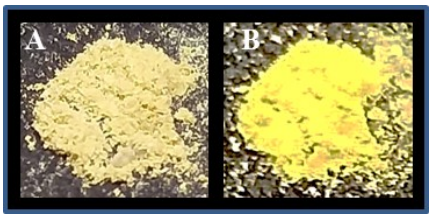

Figure S1. Images for probe molecule **TPE-Lac** (A) at normal light and (B) under UV light (long UV-365 nm). The probe **TPE-Lac** synthesized was yellow solid with bright greenish-yellow fluorescence.

2. UV-Vis spectrum for the probe TPE-Lac

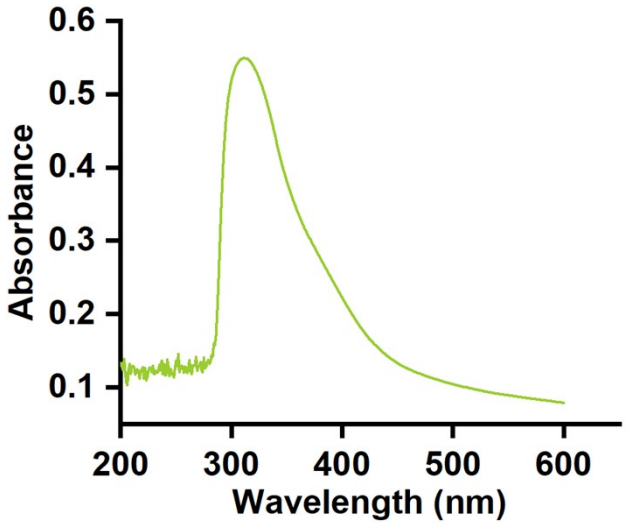

Figure S2. UV-vis spectra for the probe **TPE-Lac** (10 μM) in THF. The UV-vis showed two peaks at 312 nm and 362 nm.

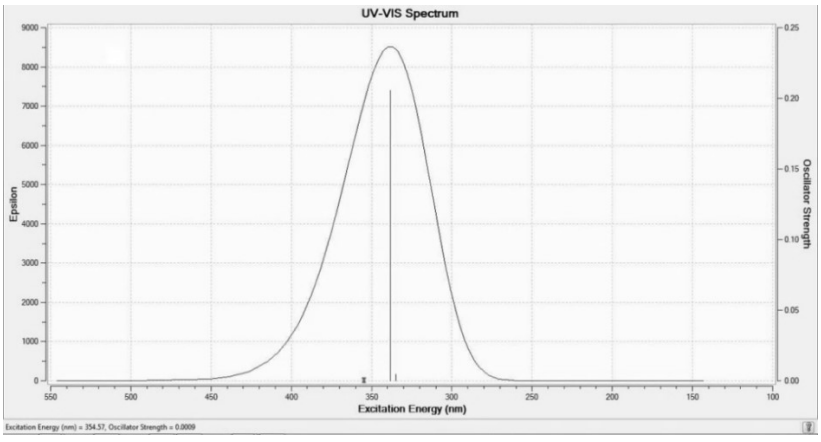

Figure S3. UV-Vis spectra predicted from the ZINDO/CI level of study for the probe **TPE-Lac**.

From the ZINDO/CI level of study, the probe **TPE-Lac** was predicted to have a peak at 339 nm with oscillator strength of 0.0009. The predicted major absorption peak (only the one beyond 300 nm) from the ZINDO/CI level of study is pretty close to the experimentally observed value.

3. Solvent study of the probe TPE-Lac

The probe **TPE-Lac** being insoluble in water, its AIE characteristic was determined by carrying out fluorescence studies in variable ratio of water-THF solvent system. It was found that probe starts fluorescing at and above 80% H_2O-THF solvent system and shows strong fluorescence at 97% H_2O-THF due to its AIE property.

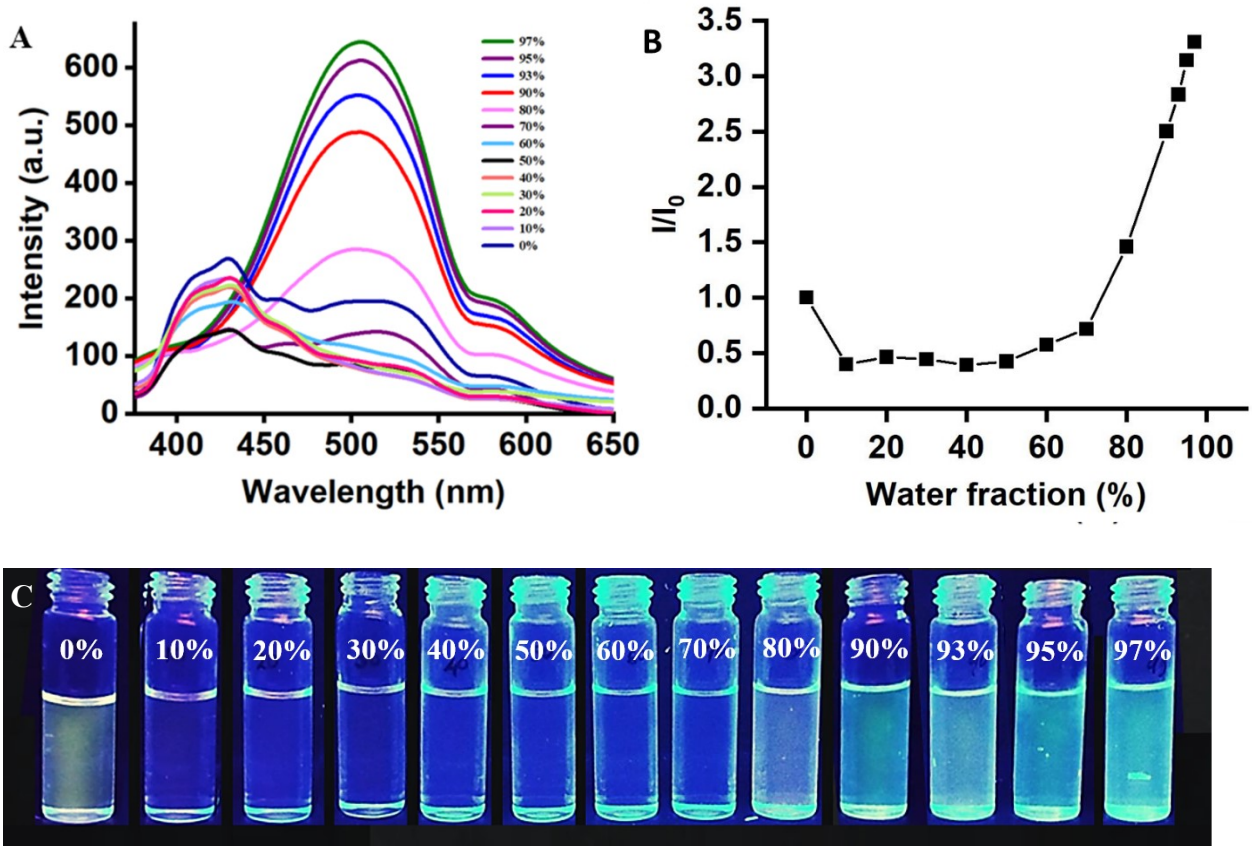

Figure S4. (A) Fluorescence response of probe **TPE-Lac** upon increasing concentration of water fraction in THF (λ_{ex} 345 nm, λ_{em} 510 nm). (B) A plot of fluorescence intensity of **TPE-Lac** against variable proportions of H_2O−THF mixture (λ_{ex} 345 nm, λ_{em} 510 nm). The probe starts showing strong AIE property at and above 80% H_2O-THF solvent system. (C) Vials from left to right represents emission of TPE-Lac (20 μM) in 0 to 97% water/THF fractions.

4. Microscopic images of the probe TPE-Lac

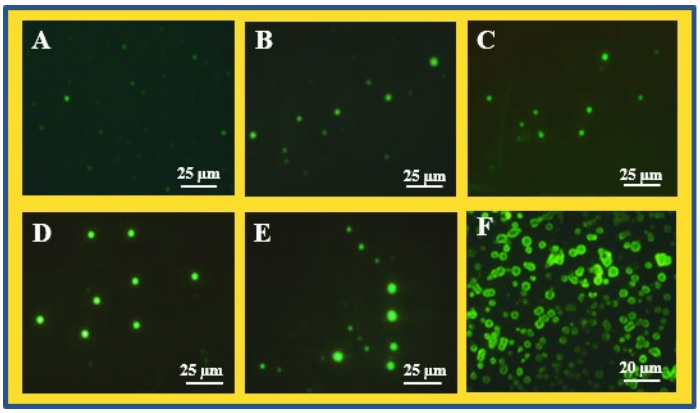

Figure S5. Microscopic images of the probe **TPE-Lac** (A) 70%, (B) 80%, (C) 90%, (D) 93%, (E) 95%, and (F) 97% water/THF fractions on glass slide (all the images were taken using FITC filter).

5. Cytotoxicity study

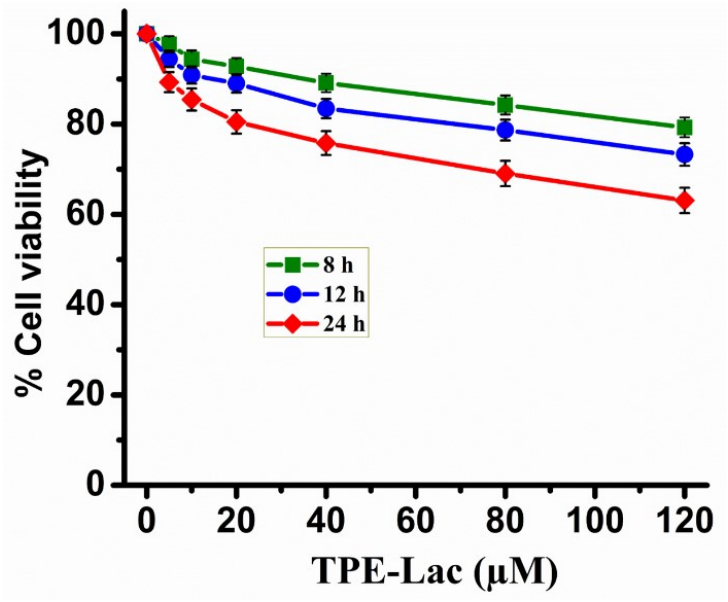

Figure S6. Plot of % cell viability of H520 cells vs the concentration of probe **TPE-Lac** after incubation of 8, 12 and 24 h, respectively.

6. Time dependent study for cyanide ion detection

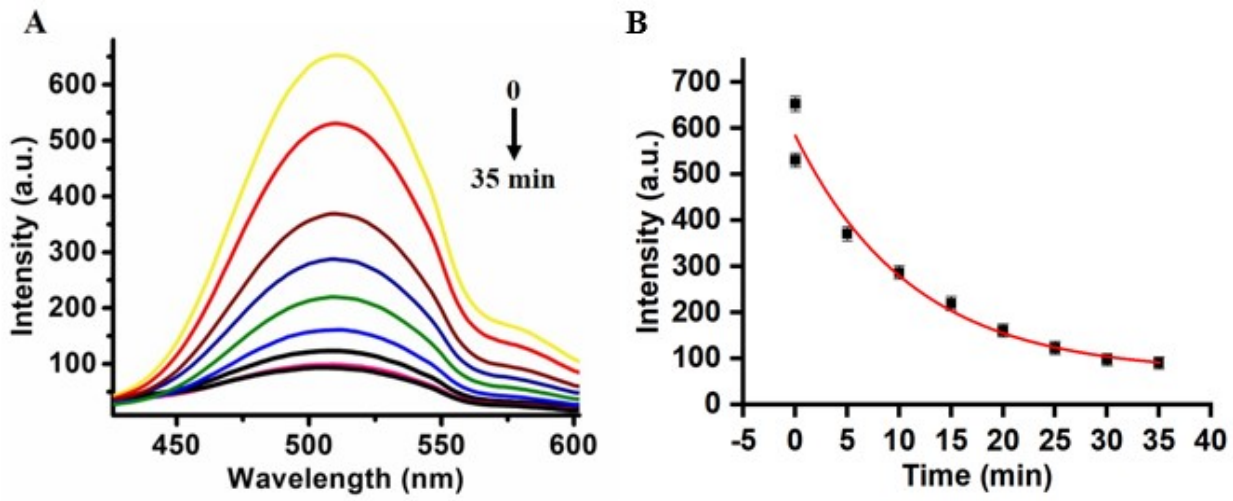

Figure S7. (A) Time-dependent fluorescence response of probe molecule **TPE-Lac** with the addition of 25 μM of cyanide anion (λ_{ex} 345 nm, λ_{em} 510 nm). (B) The plot of fluorescence emission of TPE-Lac solution with 25 μM of CN^- against time.

7. Selectivity study

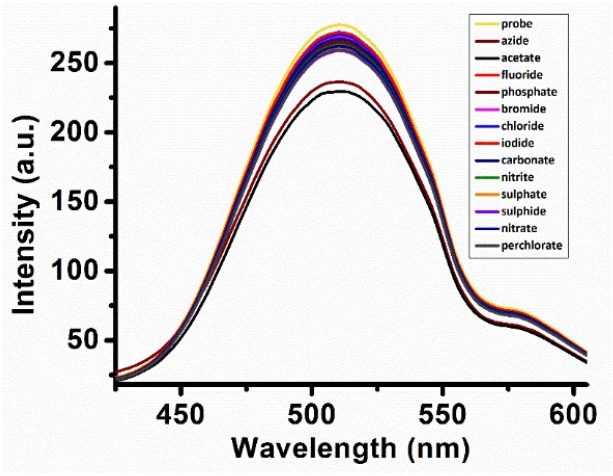

Figure S8. Fluorescence response of **TPE-Lac** upon addition of different anions (100 μM, λ_{ex} 345 nm, λ_{em} 510 nm).

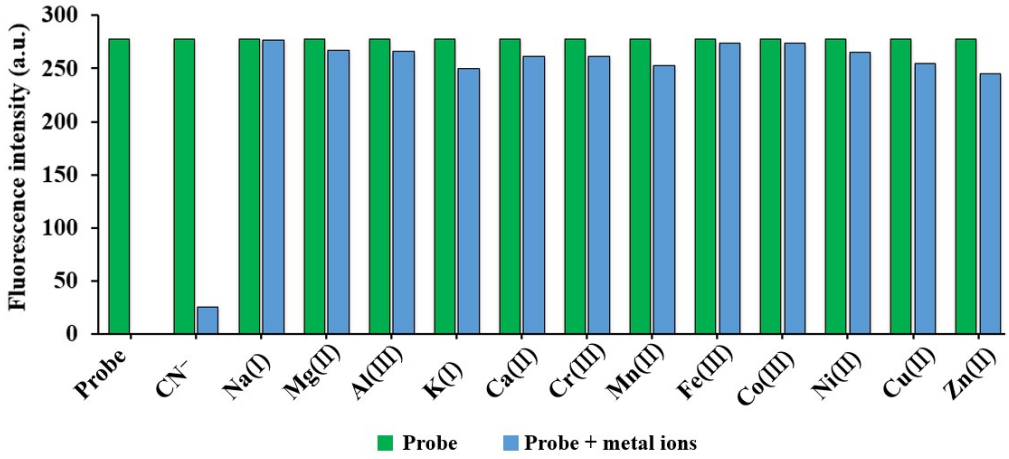

Figure S9. Fluorescence response of **TPE-Lac** upon addition of different cations (100 μM, λ_{ex} 345 nm, λ_{em} 510 nm).

8. UV study of TPE-Lac-CN$^-$ complex

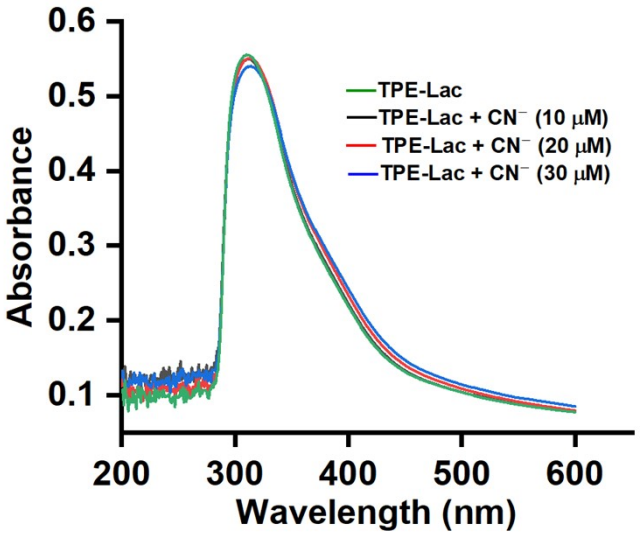

Figure S10. UV response of probe **TPE-Lac** upon addition of cyanide (upto 30 μM).

9. Mechanism of cyanide sensing

Upon the gradual addition of cyanide ions the fluorescence intensity of **TPE-Lac** slowly diminishes and ultimately is quenched. The presence of a strong electron-withdrawing group in the coumarin ring makes the 4-position susceptible to nucleophilic attack by the CN^- ion. The addition of CN^- ion interrupts the intramolecular charge transfer (ICT) process occurring through the backbone of coumarin and thereby leading to decrease in fluorescence.

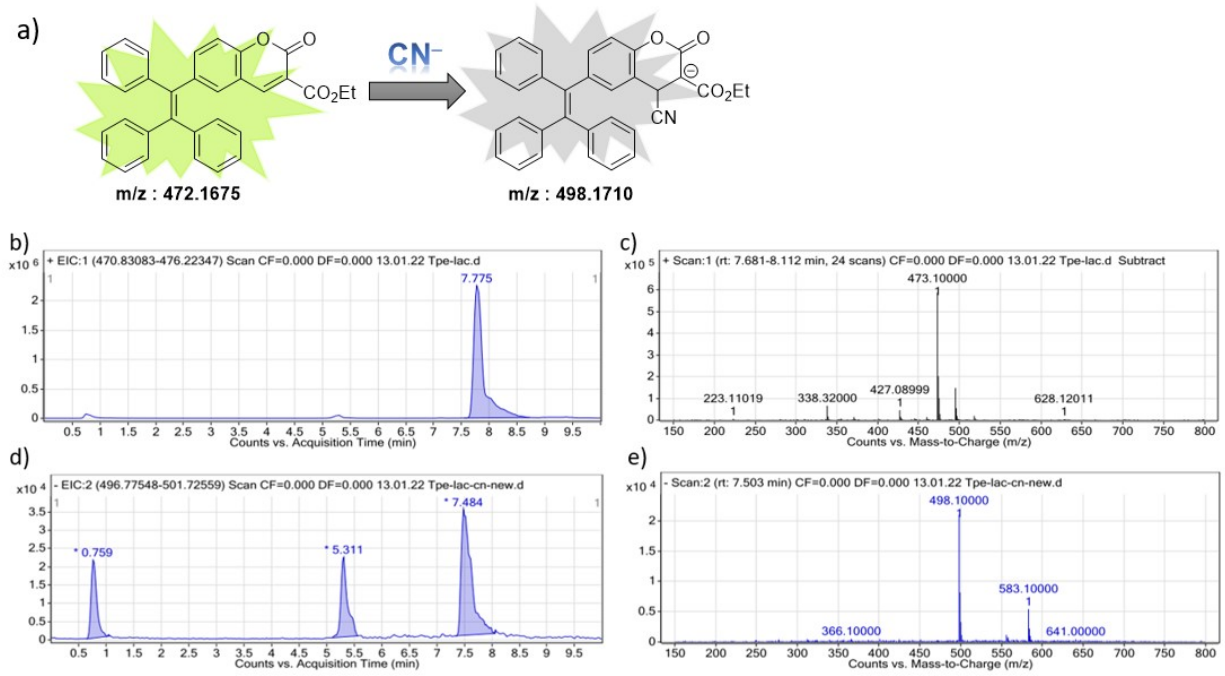

Figure S11. a) Schematic representation of sensing mechanism of cyanide using **TPE-Lac**. LCMS spectrum of probe **TPE-Lac** (b and c) before and (d and e) after addition of 1 equiv of cyanide.

10. Nitroaromatics detection

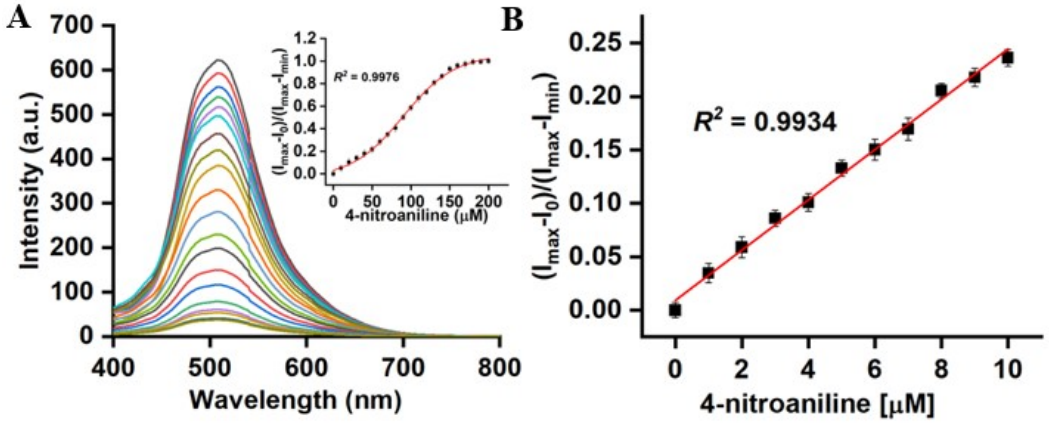

Figure S12. A) Fluorescence response of **TPE-Lac** towards 4-nitroaniline. B) Plot of fluorescence response of **TPE-Lac** against lower concentration of aniline.

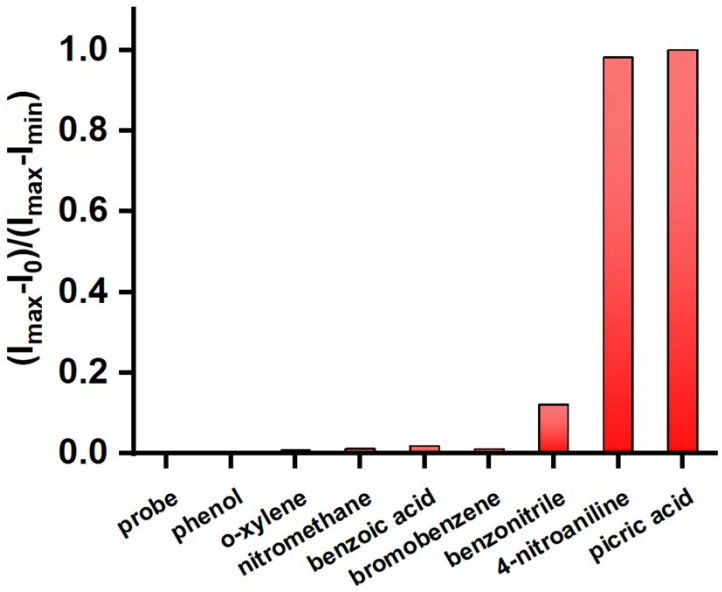

Figure S13. Selective response of **TPE-Lac** towards nitroaromatics.

Figure S14. A, C and B, D are bright field and fluorescence images of only probe **TPE-Lac** and probe **TPE-Lac** with picric acid respectively in the solution phase.

11. Table S1 Comparison of the present study and previous reports for detection of cyanide

Sr. No.	Probe Structure	Sensing method	Solvent System	Linear Range	LOD	Solid-phase study	Cell imaging	Other analytes	Ref
1	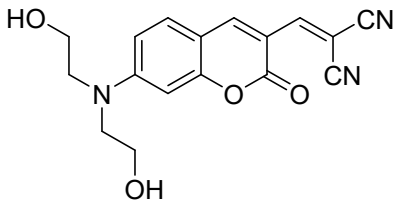 λ_{abs} = 515 nm	Colorimetric	50 % THF/HEPES, pH 7.04	-	0.8 µM.	Yes	NA	NA	S3
2	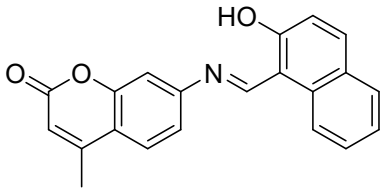 λ_{abs} = 342 nm	Colorimetric	DMSO/H_2O (8:2 v/v).	-	77.2 n M	Yes	NA	NA	S4
3	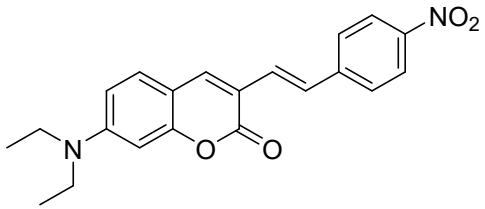 λ_{em} = 410 nm	Colorimetric and Fluorimetric	HEPES buffer (CH_3CN/ H_2O, 1:1, v/v, pH 7.4)	-	0.14 µM	Yes	NA	NA	S5

4	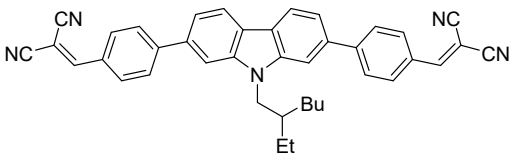 λ_{em} = 517 nm	Fluorescence turn-off	ACN:H_2O (5:95)	-	0.126 μM	Yes	NA	NA	S6
5	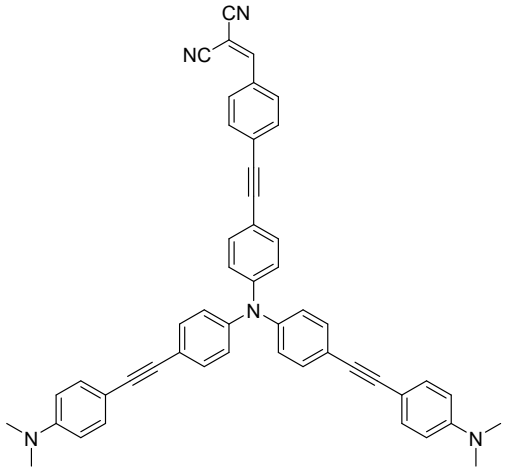 λ_{em} = 460 nm	Fluorescence turn-on	CH_3CN/ 100 mM HEPES buffer pH 10.0 (9:1 v/v)	0–80 μM	0.68 μM	NA	NA	NA	S7
6	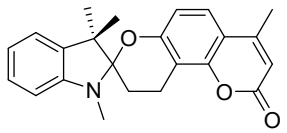	Fluorescence turn-on	Buffered water/ CH_3CN mixture (7/3	1−50 μM	1.0 μM	NA	NA	NA	S8

	λ_{em} = 453 nm		v/v; CHES 0.1 M, pH 9.6)						
7	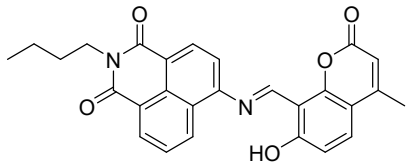 λ_{em} = 444 nm	Fluorescence turn-on	buffered water/ CH_3CN mixture (1/1 v/v; HEPES 0.1 M, pH 7.0)	-	1.8 μM	NA	Yes	NA	S9
8	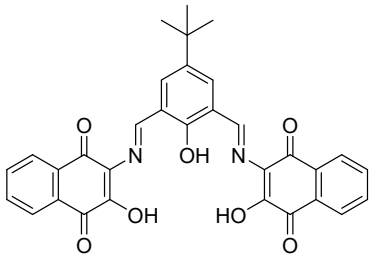 λ_{em} = 528 nm	Fluorescence turn-on	DMSO (<0.3%)/water	0–58 μM	0.6 μM	NA	NA	NA	S10
9	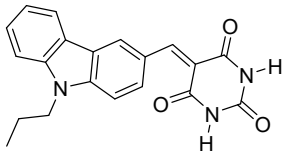 λ_{em} = 625 nm	Fluorescence Turn-off (AIE)	99% aqueous DMSO solution	0–10 μM	67.4 nM	Yes	NA	NA	S11

10	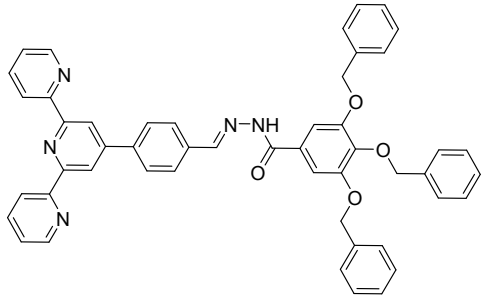 λ_{em} = 444 nm	Fluorescence turn-on (AIE)	99% aqueous DMSO solution	0–10 μM	1.09 μM.	NA	NA	NA	S12
11	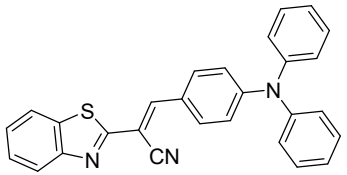 λ_{em} = 580 nm	Fluorescence turn-off (AIE)	CH_3CN/water solution (1:99, v/v),	0–5 μM	0.22 μM	Yes	Yes	NA	S13
12	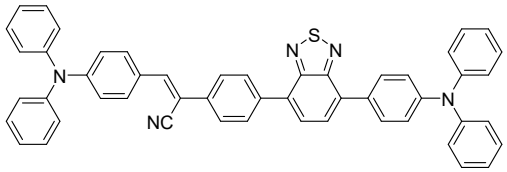 λ_{em} = 596 nm	Fluorescence turn-on (AIE)	60% DMF/PBS	0.1–1.2 μM	0.35 μM	Yes	Yes	NA	S14

13	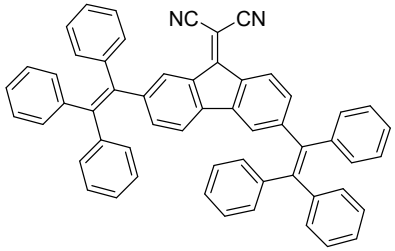 λ_{em} = 480 nm	Fluorescence turn-on (AIE)	THF:Water (10:90)	-	24.5 μM	NA	NA	NA	S15
14	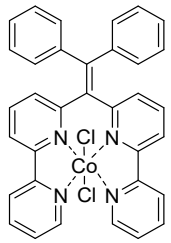 λ_{em} = 458 nm	Fluorescence turn-on (AIE)	(9:1) H_2O:MeOH	0–80 μM	0.59 μM	NA	NA	NA	S16
15	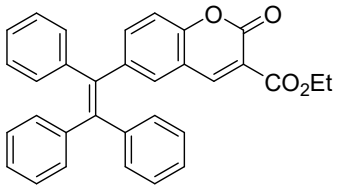 λ_{em} = 510 nm	Fluorescence turn-off AIE	THF: Water (3: 97)	0–14 μM	33 nM	Nitroaromatics	Yes	Yes	Present work

12. Reference

S1. X. F. Duan, J. Zeng, J. W. Lu and Z. B. Zhang, *J. Org. Chem.*, 2006, **71**, 9873−9876.

S2. H. T. Feng, S. Song, Y. C. Chen, C. H. Shen, and Y. S. Zheng, *J. Mater. Chem. C*, 2014, **2**, 2353–2359.

S3. X. Cheng, R. Tang, H. Jia, J. Feng, J. Qin, and Z. Li, *ACS Appl. Mater. Interfaces*, 2012, **4**, 4387−4392.

S4. Y. Leng, J. Zhang, Q. Li, Y. Zhang, Q. Lin, H. Yao and T. Wei, *New J. Chem.*, 2016, **40**, 8607–8613.

S5. X. Sun, Y. Wang, X. Zhang, S. Zhang and Z. Zhang, *RSC Adv.*, 2015, **5**, 96905–96910.

S6. R. K. Konidena and K. R. J. Thomas, *RSC Adv.*, 2014, **4**, 22902–22910.

S7. E. Thanayupong, K. Suttisintong, M. Sukwattanasinitt and N. Niamnont, *New J. Chem.*, 2017, **41**, 4058−4064.

S8. Y. Shiraishi, M. Nakamura, N. Hayashi and T. Hirai, *Anal. Chem.*, 2016, **88**, 6805−6811.

S9. Y. Shiraishi, N. Hayashi, M. Nakahata, S. Sakai and T. Hirai, *RSC Adv.*, 2017, **7**, 32304–32309.

S10. G. Mahalakshmi, P. S. Kumar, P. Rajalakshmi, M. Seenivasaperumal and K. P. Elango, *Methods Appl. Fluoresc.*, 2019, **7**, 025003.

S11. Q. Zou, F. Tao, H. Wu, W. W. Yu, T. Li and Y. Cui, *Dyes Pigm., 2019,* **164**, 165–173.

S12. A. Sebastian and E. Prasad, *Langmuir*, 2020, **36**, 10537−10547.

S13. X. Chen, L. Wang, X. Yang, L. Tang, Y. Zhou, R. Liu and J. Qua, *Sens. Actuators, B*, 2017, **241**, 1043–1049.

S14. K. Deng, L. Wang, Q. Xia, R. Liu and J. Qua, *Sens. Actuators, B,* 2019, **296**, 126645.

S15. M. H. Chua, H. Zhou, T. T. Lin, J. Wu and J. Xu, *J. Mater. Chem. C*, 2017, **5**, 12194–12203.

S16. M. T. Gabr and F. C. Pigge, *Dalton Trans.*, 2018, **47**, 2079–2085.

^{1}H NMR

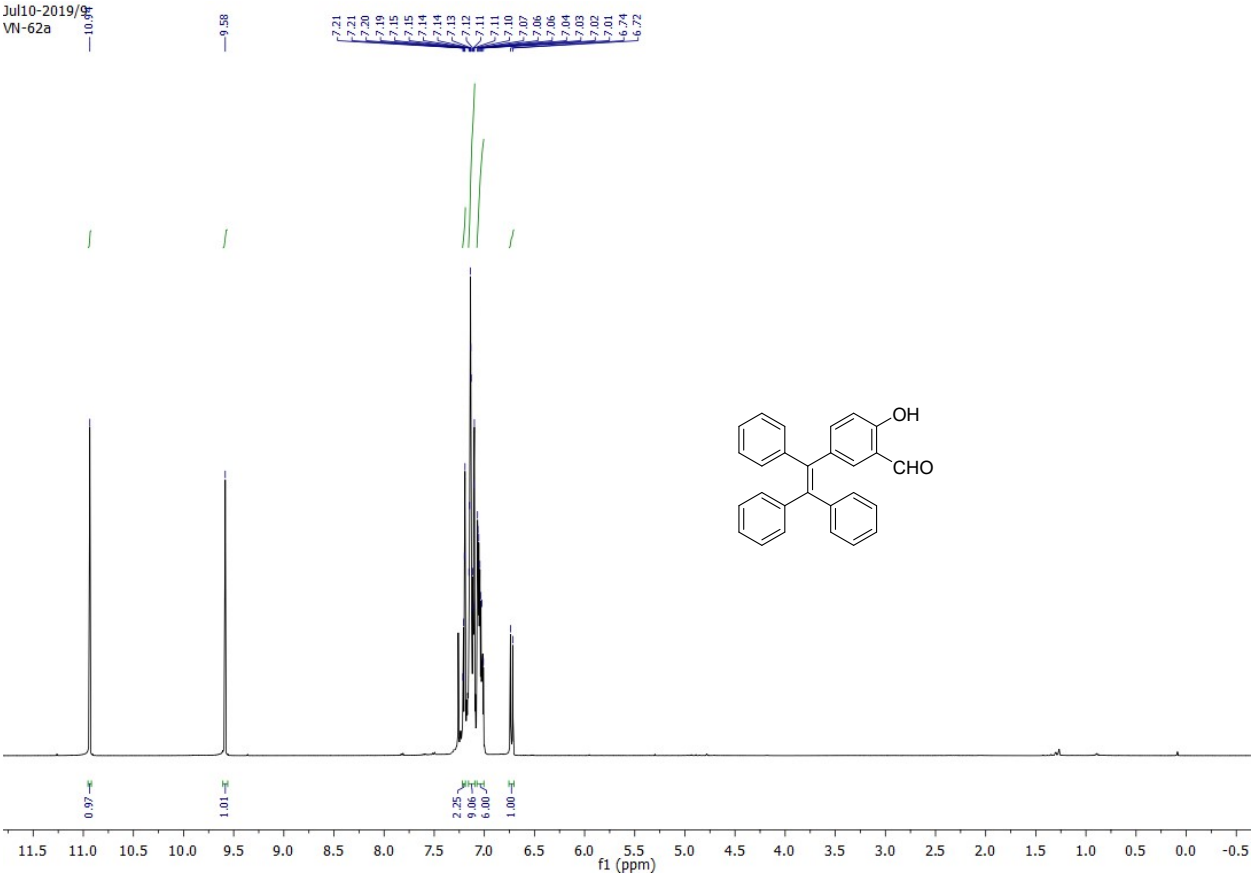

^{1}H NMR for TPE-OH-CHO (4)

^{13}C NMR

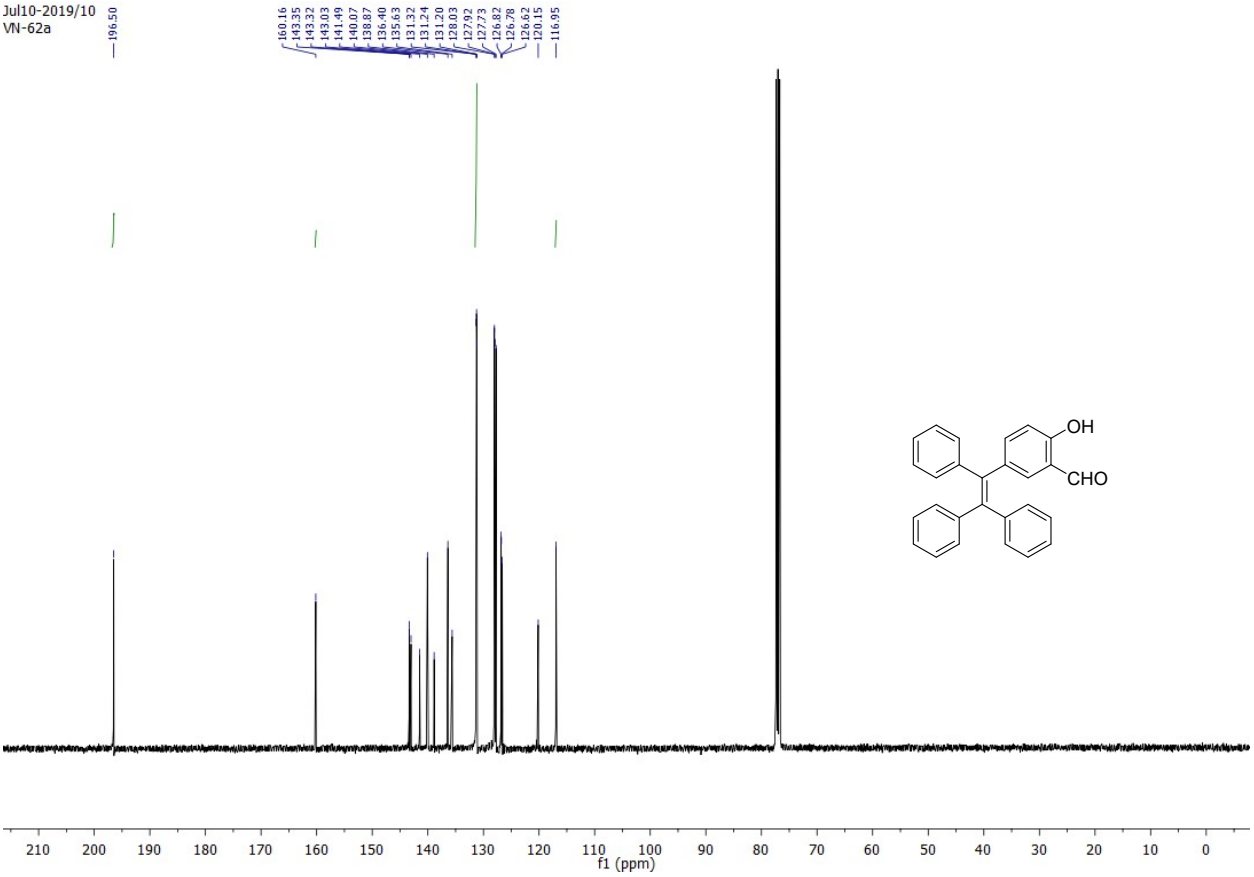

^{13}C NMR for TPE-OH-CHO (4)

^{1}H NMR

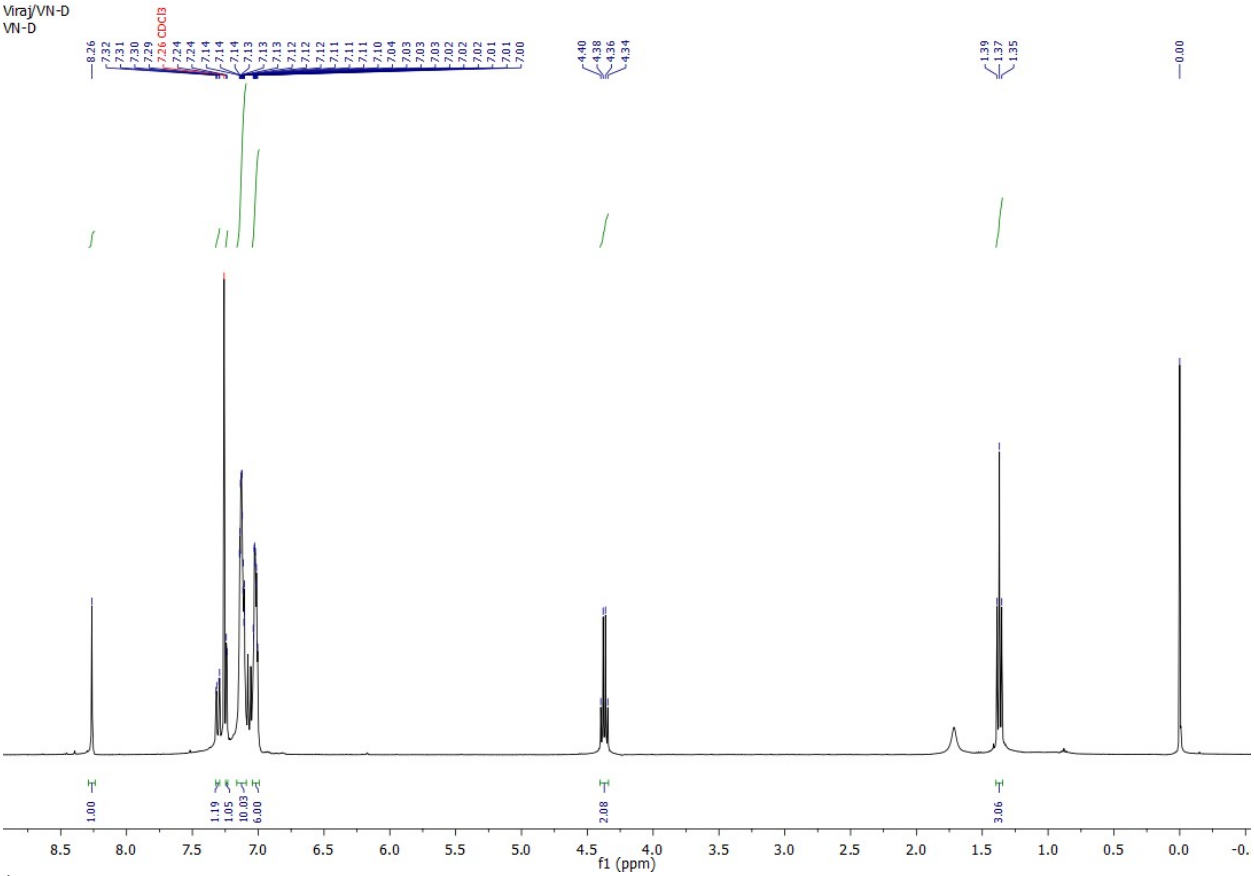

^{1}H NMR for TPE-Lac (5)

^{13}C NMR

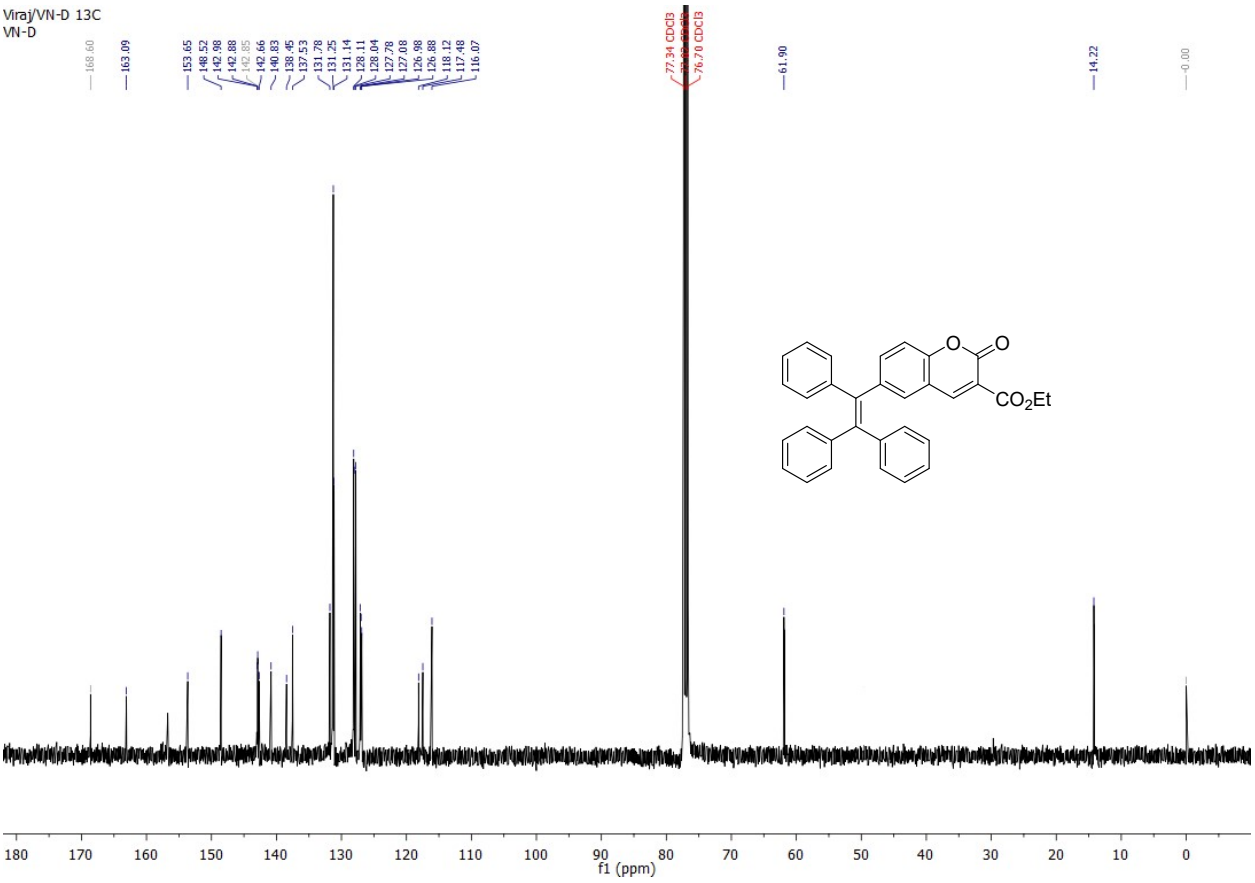

^{13}C NMR for TPE-Lac (5)

HRMS data

Compound Table

Compound Label	RT	Mass	Abund	Formula	Tgt Mass	Diff (ppm)
Cpd 1: 0.182 99.0551	0.182	376.1467	15418	C27 H20 O2	376.1463	0.9

Compound Label	*m/z*	RT	Algorithm	Mass
Cpd 1: 0.182 99.0551	377.1538	0.182	Find By Formula	376.1467

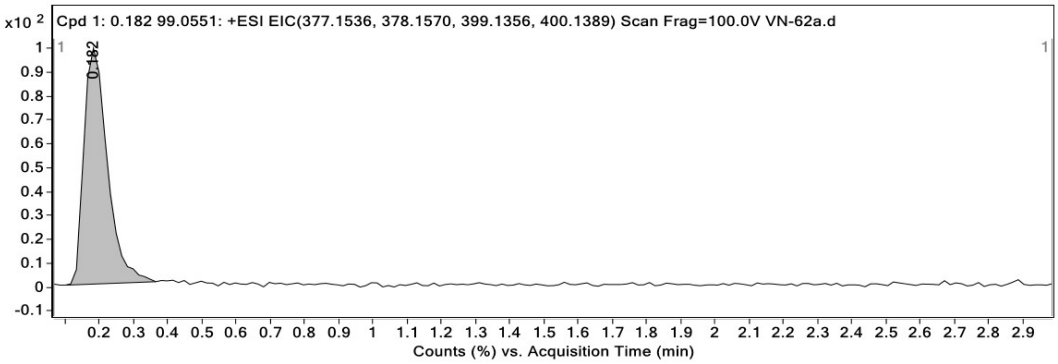

Liquid chromatograph for TPE-OH-CHO (4)

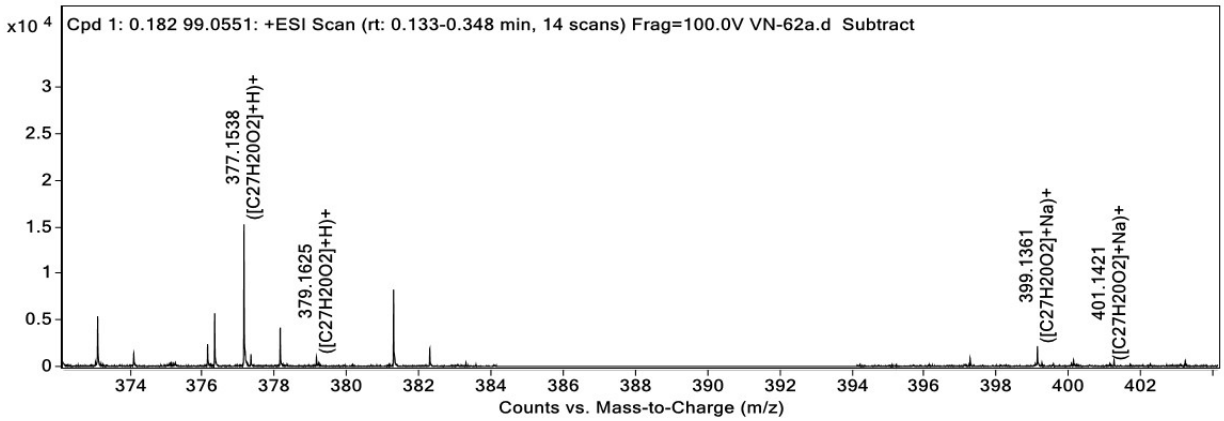

Mass spectrum for TPE-OH-CHO (4)

Compound Table

Compound Label	RT	Mass	Abund	Formula	Tgt Mass	Diff (ppm)
Cpd 1: 0.188 495.1567	0.188	473.1712	112630	C32 H25 O4	473.1753	-8.73

Compound Label	*m/z*	RT	Algorithm	Mass
Cpd 1: 0.188 495.1567	474.178	0.188	Find By Formula	473.1712

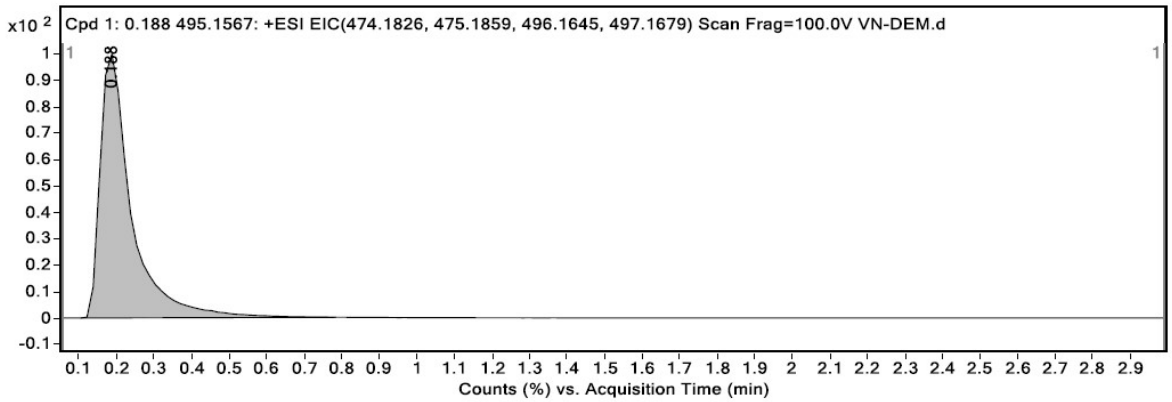

Liquid chromatograph for TPE-Lac (5)

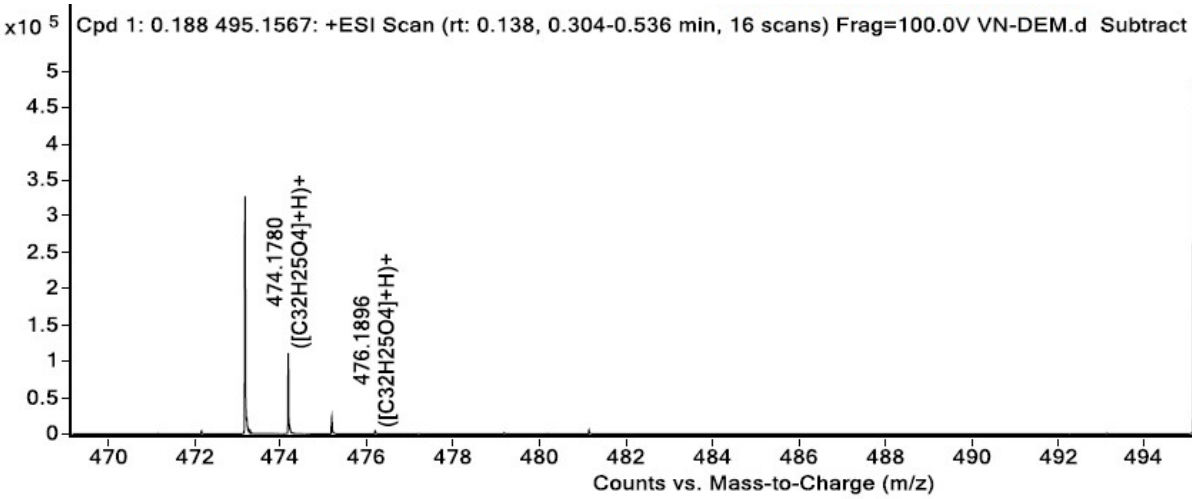

Mass spectrum for TPE-Lac (5)

IR spectra

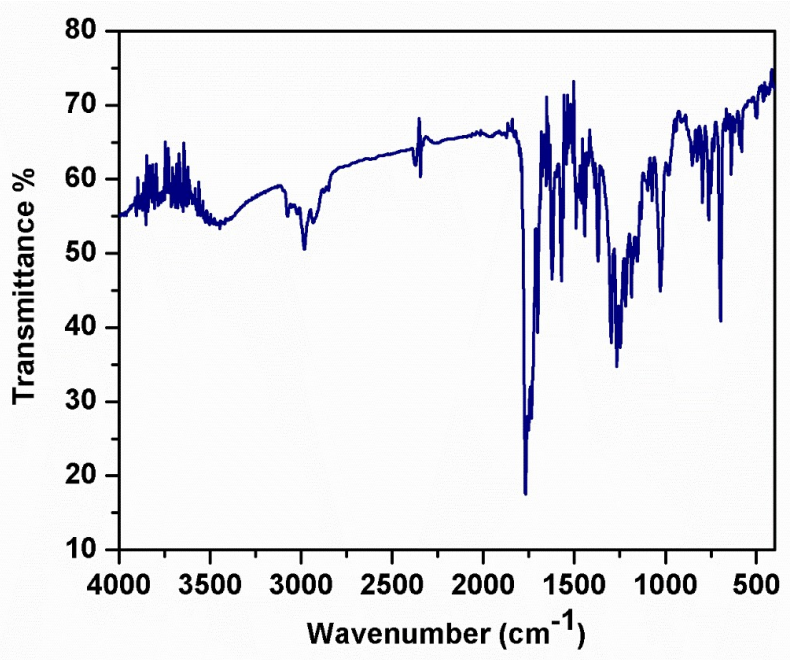

IR for TPE-Lac (5)